Title: Robust and stable transcriptional repression in *Giardia* using CRISPRi

*McInally SG, *Hagen KD, Nosala C, Williams J, Nguyen K, Booker J, Jones K, and Scott C. Dawson

*These authors contributed equally to this work

Department of Microbiology and Molecular Genetics

One Shields Avenue

UC Davis

Davis, CA 95616

Corresponding author: scdawson@ucdavis.edu

Running Title: CRISPRi in *Giardia*

Keywords: *Giardia*, CRISPR/Cas9, CRISPRi, kinesin

ABSTRACT

Giardia is a widely prevalent yet understudied protistan parasite causing significant diarrheal disease worldwide. Despite the availability of several sequenced genomes, basic and applied *Giardia* research has lagged behind other parasites due to a lack of molecular genetic tools for functional genomic research. While used extensively in other non-model eukaryotes, the adaptation of CRISPR/Cas9-mediated genome editing has been challenging in *Giardia* due to two transcriptionally-active diploid nuclei, the lack of a non-homologous end-joining (NHEJ), few positive selectable markers, and an inability to target Cas9 to both nuclei. Yet precise, stable, and tunable transcriptional repression is also an essential tool to interrogate gene function. CRISPR interference (CRISPRi) is a modification of the CRISPR/Cas9 system using a catalytically inactive Cas9 (dCas9) to induce gene knockdowns by site-specific transcriptional repression. CRISPRi is stable, modular, inducible, and reversible and thus has significant advantages over existing transient methods of gene disruption in *Giardia*. To adapt CRISPRi, we first defined a native *Giardia* nuclear localization signal (NLS) that is necessary and sufficient to target Cas9 or dCas9 to both nuclei. CRISPRi-mediated knockdown using single or multiple gRNAs allowed us to efficiently and stably repress one exogenous reporter gene and three endogenous cytoskeletal genes important for pathogenesis. Each endogenous gene knockdown had significant flagellar or ventral disc defects indicating that *Giardia* CRISPRi is robust, stable and flexible method of transcriptional repression. This tunable knockdown strategy will transform molecular genetic studies in *Giardia*, permitting the targeted knockdown of one or more genes, as well genome-scale functional genetic profiling.

IMPORTANCE

Giardia is a human parasite that causes diarrheal disease in several hundred million people each year, particularly in areas that lack adequate clean water and sanitation. Due to growing evidence of resistance, there is a need for new effective and affordable treatments. *Giardia* research has been limited by our ability to genetically manipulate the parasite genome to study gene function. To aid in our understanding of how *Giardia* infection causes disease, we adapted a genetic method to modify gene expression in *Giardia*. We demonstrated the use of this method to deplete the *Giardia* cell of several proteins important for its pathogenesis, and these depletions resulted in severe cellular defects. The widespread use of these new genetic tools will finally allow us to test the roles of proteins important for pathogenesis, which is a key step in anti-*Giardia* drug development.

INTRODUCTION

Giardia lamblia is a common parasitic protist that infects over three hundred million people worldwide each year, causing acute diarrheal disease in areas with inadequate sanitation and water treatment (1-3). The need for new effective and affordable treatments for giardiasis is underscored by estimated failure rates of up to 20% for standard treatments (4), emerging evidence of drug resistance (5-7), and the prevalence of chronic or recurrent infections (8). Giardiasis is considered a neglected disease due to its wide prevalence and to a general lack of understanding of parasite biology and interactions with the host at the molecular and cellular levels (1).

Giardia has a two-stage life cycle in which mammalian hosts ingest cysts from contaminated sources. Cysts then excyst into motile, binucleate trophozoites after passage through the stomach. Trophozoites attach extracellularly to the gut epithelium, proliferate, and later differentiate back into infectious cysts that are excreted (9). Each nucleus of the trophozoite is diploid (10) and transcriptionally active (11). Genome sequencing of several assemblages of *Giardia*, supports that both nuclei have equivalent genetic content (12-15).

The development of molecular genetic tools such as CRISPR/Cas9-mediated genome editing in *Giardia* has been considerably slower than for other parasitic protists (16-19) or other polyploid organisms (20, 21), because *Giardia* is essentially polyploid, lacks a non-homologous end-joining (NHEJ) pathway (15), and lacks a defined sexual cycle (22). In addition, the single SV40 NLS used for nuclear localization of other *Giardia* proteins (23) is not sufficient to target native

Streptomyces pyogenes Cas9 (spCas9) to *Giardia's* nuclei (24). Finally, the rudimentary understanding of transcription factors and promoters (25) and a limited number of selectable markers (20, 21) (26) contributed to the slow pace of molecular genetic tool development in *Giardia*. For these reasons, the first *Giardia* quadruple knockout strain of a component of the cyst wall (CWP1) was made using a Cre/LoxP strategy to recycle selectable markers in a heroic effort that took over two years (24).

Gene knockouts are only one of many strategies to interrogate gene function (27), and null alleles in essential processes like cell cycle regulation (28) and cytokinesis (29) can result in severely reduced fitness or lethality. Precise, stable, and tunable transcriptional repression and overexpression are alternative, yet essential, tools for the systematic characterization of gene function. Despite the presence of conserved components of the RNAi machinery, RNAi does not efficiently silence genes in *Giardia* (30). Translational repression using morpholino oligonucleotides has been used extensively in *Giardia* (31-35), but morpholino knockdowns are transient (lasting less than 48 hours), can lack complete penetrance, and are less amenable to genome-wide functional screens due to the high cost associated with each morpholino (30). Furthermore, the transience and penetrance of the morpholino knockdown is not optimal for characterization of *in vivo* infection dynamics (36).

CRISPR/Cas9 is a modular and flexible DNA-binding platform for the recruitment of proteins to a target DNA sequence and has thus been adapted for other uses beyond genome editing (37). The CRISPR interference system (CRISPRi) is a modification of the CRISPR/Cas9 system using a

catalytically inactive (dead Cas9, dCas9) to induce stable, inducible, or reversible gene knockdown in human cell lines and yeast (37), as well as diverse bacteria (37-42). Like Cas9, the inactive dCas9 is directed to precise genomic targets using a complementary guide RNA (gRNA). However, upon binding, the inactive dCas9/gRNA complex inhibits transcription initiation and/or elongation rather than inducing double-stranded breaks in DNA (37).

CRISPRi has significant advantages over RNAi or morpholinos as CRISPRi directly and stably inhibits transcription (37). As a modular and exogenous system, CRISPRi does not interfere with endogenous microRNA expression or function (37), and because CRISPRi acts at the DNA level, *Giardia* noncoding RNAs (43), microRNAs (44, 45), antisense transcripts (46), and polymerase III transcripts (47) could be targeted for repression. In diverse bacteria, yeast, and human cell lines, CRISPRi is empirically as effective as RNAi in transcriptional silencing with significantly fewer off-target effects (37).

Here we demonstrate efficient, stable, and modular CRISPRi-mediated transcriptional repression in *Giardia* of both endogenous and exogenous genes. This first successful application of CRISPRi for transcriptional knockdown in a parasitic protist—or a polyploid eukaryote—highlights the utility of CRISPRi for emerging model systems in any domain of life. First, we define a native *Giardia* nuclear localization signal (NLS) that is both necessary and sufficient to target Cas9 to both nuclei. We then develop and use CRISPR interference to efficiently and stably repress one exogenous reporter gene, and three endogenous *Giardia* cytoskeletal genes important for pathogenesis. The efficiency and simplicity of CRISPRi in *Giardia* permits the rapid

assessment of the phenotypic consequences of protein knockdown (37, 48) and will likely enable the first forward and reverse genetic screens.

METHODS

Construction of expression vectors Cas9-SV40NLS and Cas9-SV40NLS-GFP

Expression vector Cas9-SV40NLS-GFP was constructed by placing mammalian codon-optimized Cas9 (mCas9) with a C-terminal SV40 nuclear localizing signal (NLS) from JDS246 (Addgene #43861, JK Joung, unpublished) under the control of the *Giardia* malate dehydrogenase (MDH; GiardiaDB GL50803_3331) promoter. A 3xHA epitope tag widely used in *Giardia* (26) was added to the C-terminal end and the resulting PMDH-mCas9-SV40NLS-3HA fragment was cloned into our C-terminal GFP vector, pcGFP1Fpac (49), fusing Cas9 to GFP. Deletion of the GFP tag produced expression vector Cas9-SV40NLS.

Identification of putative Giardia NLSs and construction of vectors to test NLS efficacy

Putative NLS sequences were identified among the protein sequences of 65 *Giardia* strains expressing C-terminal GFP-tagged proteins that localize to the nuclei (50) using the NLS prediction software NLStradamus (51), with the two state HMM static model and posterior prediction with a cutoff of 0.6. To delete NLSs, we amplified protein coding regions plus 200 bp of upstream sequence to include native promoters using reverse primers that excluded the NLSs and any downstream sequence, and cloned the truncated fragments into pcGFP1Fpac (49). NLS sequences were added to Cas9 either by replacing the GFP tag in Cas9-SV40NLS-GFP with the NLS sequence to be tested (for C-terminal NLSs), or by adding a new start codon and

NLS in front of the start codon of Cas9 (for N-terminal NLSs). NLS sequences were generated by PCR amplification from genomic DNA or by annealing short complementary oligonucleotides.

Construction of dCas9 CRISPR interference vector dCas9g1pac

dCas9g1pac was created by amplifying the GL50803_2340 NLS from *Giardia* genomic DNA with 2340NLSAgeF (5'-actgctaccggtcctcccagagaagaagcggtccaag-3') and 2340NLSNotIR (5'-actgctgcggccgctttagctcttaattttactaactctacgatcc-3') and cloning it into Cas9-SV40NLS-GFP to replace GFP. A gRNA expression cassette with inverted BbsI sites for cloning gRNAs was added, followed by the gRNA scaffold sequence from pX330 (52). To drive gRNA expression in *Giardia* and ensure proper termination, we included approximately 200 bp of DNA located upstream and downstream of the *Giardia* U6 spliceosomal snRNA (47). The upstream sequence includes 12 bp of U6 coding sequence, and the downstream sequence includes the 12 bp motif thought to mediate 3' end processing (47). The gRNA cassette was synthesized (Biomatik) and inserted into a unique Acc65I site in the vector. The dCas9 mutations D10A and H840A were added by replacing a 3.6 kb NcoI-NheI fragment within Cas9 with a similar fragment from dCas9 vector MSP712 (Addgene #65768) (53).

Guide RNA design and cloning

Specific guide RNAs (20 nt) were designed with the CRISPR 'Design and Analyze Guides' tool from Benchling (https://benchling.com/crispr) using a NGG PAM sequence and the *Giardia lamblia* ATCC 50803 genome (GenBank Assembly GCA_000002435.1). gRNAs were designed to target the non-template strand unless otherwise specified (Table S1). gRNA oligonucleotides

with 4-base overhangs complementary to the vector sequence overhangs were annealed and cloned into BbsI-digested dCas9g1pac. To express two gRNAs, each was individually cloned and then a universal primer set (gRNA_multiplex_F: 5'-gtcttataaggtaccgagcttgattgcaatagcaaacag-3' and gRNA_multiplex_R: 5'-ctatagggcgaattcgagctgagctcggtaccttataagacaacatc-3') was used to amplify the entire gRNA cassette from one plasmid and insert it into the SacI site of the second via Gibson assembly (54). This method was also used to generate the control plasmid dCas9g2pac, which has two empty gRNA cassettes. While we have only used two gRNAs here, this method regenerates the SacI restriction site, allowing the insertion of additional gRNAs using the same primers (Table S1).

Construction of the NanoLucNeo luciferase expression vector

The NanoLucNeo vector was constructed via PCR amplification of IFT81 (GiardiaDB GL50803_15428), the MDH promoter (GiardiaDB GL50803_3331), and NanoLuc (pFN31K, Promega). The resulting amplicons were cloned via Gibson assembly into BamHI and EcoRI digested pKS_mNeonGreen-N11_NEO (29).

Strains and culture conditions

All *G. lamblia* (ATCC 50803) strains were cultured in modified TYI-S-33 medium supplemented with bovine bile and 5% adult and 5% fetal bovine serum [56] in sterile 16 ml screw-capped disposable tubes (BD Falcon), and incubated upright at 37°C without shaking. Vectors were introduced into WBC6 or NanoLucNeo trophozoites by electroporation (roughly 20 µg DNA) as previously described (49). Strains were maintained with antibiotic selection (50 µg/ml

puromycin and/or 600 µg/ml G418) (49). All CRISPRi strains were thawed from frozen stocks and cultured for 24 to 48 hours prior to phenotypic analysis.

Quantitation of transcriptional knockdown using quantitative PCR (QPCR)

RNA was extracted using a commercial kit (Zymo Research). RNA quality was assessed by spectrophotometric analysis and electrophoresis prior to double-stranded cDNA synthesis using the QuantiTect Reverse Transcription Kit (Qiagen). Quantitative PCR of kinesin-2a (GiardiaDB GL50803_17333) was performed using 17333_qPCR1F 5' GCCTCAACCAACTACGACGA 3' and 17333_qPCR1R 5' TCAGCACATCCATCGGCTTT 3'. Quantitative PCR of kinesin-13 (GiardiaDB GL50803_16945) was performed with 16945_qPCR3F 5' CCAATACGCTGCAAAGCCTC 3' and 16945_qPCR3R 5' AGCCAGTTTGTCCATACGCA 3'. Analyses were performed using SensiFast No-ROX SYBR-green master mix (Bioline) in an MJ Opticon thermal cycler, with an initial two-minute denaturation step at 95°C followed by 40 cycles of 95 °C for 5 seconds, 60°C for 10 s, and 72 °C for 10 s. The constitutively expressed gene for glyceraldehyde 3-phosphate dehydrogenase (GAPDH, GiardiaDB GL50803_ 6687) was chosen as an internal reference gene and was amplified with gapdh-F 5' CCCTTCACGGACTGTGAGTA 3' and gapdh-R 5' ATCTCCTCGGGCTTCATAGA 3' (36). Ct values were determined using the Opticon Monitor software and statistical analyses were conducted using custom Python scripts. All qPCR experiments were performed using two biologically independent samples with four technical replicates. Data is shown as mean expression relative to the GAPDH control sample with 95% confidence intervals.

In vitro bioluminescence assays of NanoLuc knockdown strains

Giardia trophozoites were grown to confluency at 37°C for 48 hours, iced for 15 minutes to detach trophozoites and centrifuged at 900 x g for five minutes at 4°C. Trophozoites were resuspended in 1 ml of cold media and serial dilutions (10^{-1}, 10^{-2}) were made for enumeration using a hemocytometer. To measure luminescence, three 50 µl aliquots of the 10^{-2} dilution (approximately 10^3 cells) were loaded into a white opaque 96-well assay plate (Corning Costar) and incubated for 30 minutes at 37°C. Following incubation, 50 µl of Nano-Glo® Luciferase assay reagent (Promega), prepared at a 1:50 ratio of substrate to buffer, was added to each well. Luminescence was analyzed on a VictorX3 plate reader warmed to 37°C, using 0.1-second exposures, repeated every 30 seconds until maximal signal was detected. Experiments were performed using three technical replicates that were averaged over three different luminescence acquisitions and displayed with 95% confidence intervals. To determine the linear dynamic range of detection for the NanoLucNeo strain, we used tenfold serial dilutions and plotted the luminescence readings versus the number of cells loaded into each well (Figure S2).

Immunostaining of Cas9 and dCas9 CRISPRi strains

Giardia trophozoites grown to confluency were harvested (see above), washed twice with 6 ml of cold 1X HBS and resuspended in 500 µl of 1X HBS. Cells (250 µl) attached to warm coverslips (37°C, 20 min) were fixed in 4% paraformaldehyde, pH 7.4 (37°C, 15 min), washed three times with 2 ml PEM, pH 6.9 (35), incubated in 0.125M glycine (15 min, 25°C), washed three more times with PEM, and permeabilized with 0.1% Triton X-100 for 10 minutes. After three additional PEM washes, coverslips were blocked in 2 ml PEMBALG (35) for 30 minutes and

incubated overnight at 4°C with anti-TAT1 (1:250), anti-HA (1:500, Sigma), mouse anti-Cas9 (1:1000, Abcam), anti-Beta-Giardin (1:1000) and/or rabbit anti-Cas9 (1:1000, EpiGentek) antibodies. Coverslips were then washed 3 times in PEMBALG and incubated with Alex Fluor 488 goat anti-rabbit and/or Alex Fluor 594 goat anti-mouse antibodies (1:250; Life Technologies) for two hours at room temperature. Coverslips were washed three times each with PEMBALG and PEM and mounted in Prolong Gold antifade reagent with DAPI (Life Technologies).

Flagellar pair length measurements and ventral disc phenotype analysis

Serial sections of immunostained trophozoites were acquired at 0.2 µm intervals using a Leica DMI 6000 wide-field inverted fluorescence microscope with a PlanApo ×100, 1.40 numerical aperture (NA) oil-immersion objective. For flagellar pair length measurements, DIC images were analyzed in FIJI (55) using a spline-fit line to trace the flagella from the cell body to the flagellar tip. Trophozoites with colocalized DAPI and anti-Cas9 signal were evaluated as positive for dCas9 expression, while cells with undetectable colocalization were considered dCas9 negative. For analysis of ventral disc phenotypes, the proportion of aberrant ventral discs and dCas9-positive nuclei within a field of view was determined from maximum intensity projections of processed images. Data were analyzed, and figures were generated using custom Python scripts. Data is shown as mean relative length changes with 95% confidence intervals.

Super-resolution images of trophozoites exhibiting phenotypes typical of median body protein (MBP, GL50803_16343) silencing by dCas9 were collected at 0.125 µm intervals on a Nikon N-

SIM Structured Illumination Super-resolution Microscope with a 100x, 1.49 NA objective, 100 EX V-R diffraction grating, and an Andor iXon3 DU-897E EMCCD. Images were reconstructed in the "Reconstruct Slice" mode and were only used if the reconstruction score was 8. Raw and reconstructed image quality were further assessed using SIMcheck (56); only images with adequate scores were used for analysis. Images are displayed as a maximum intensity projection.

RESULTS

The SV40 NLS is not sufficient to localize Cas9 to the two Giardia nuclei

To express Cas9 in *Giardia*, we cloned mammalian-codon optimized *Streptococcus pyogenes* Cas9 (mCas9) with a C-terminal SV40 nuclear localization signal (NLS) and a 3XHA epitope tag into the pcGFP1Fpac backbone (57), creating a Cas9-SV40NLS-3HA-GFP fusion (Figure 1A). A comparison of the modal codon usage frequencies (58) of mCas9 and all protein coding genes of *Giardia lamblia* ATCC 50803 indicated that further codon optimization of mCas9 was unnecessary. As Cas9 toxicity has been reported in some systems (59), Cas9 was expressed using a moderate-strength *Giardia* promoter for the constitutive malate dehydrogenase (MDH, GL50803_3331) gene (Figure 1A).

The Cas9-SV40NLS-GFP fusion localized only to the cytoplasm, with no signal detected in either of the nuclei (Figure 1A). Cas9 localization to the nucleus is required for Cas9 genome editing, therefore we added a second SV40 NLS at the N-terminus. However, addition of another SV40 NLS had no impact on nuclear localization (Figure 1A). Thus, the SV40 NLS, which is commonly

used in other systems and for rCas9 in commercial Cas9/CRISPR kits, is not sufficient for nuclear localization of Cas9 in *Giardia*. The failure of the SV40 NLS to target full length Cas9 to *Giardia's* nuclei has been noted previously, although a truncated and inactive Cas9 was successfully localized with this NLS (24), as were GFP and TetR (23).

Defining a native Giardia NLS to target Cas9 and dCas9 to both nuclei

To determine whether the predicted NLS regions (51) were necessary for nuclear localization (see Methods), we deleted putative C-terminal NLS sequences from seven nuclear-localizing GFP tagged *Giardia* proteins and assayed for loss of nuclear localization (Figure 1B and S1). Deletion of NLSs resulted in the loss of localization to the nuclei and/or an increase in localization to the cytoplasm for three strains (Figure 1B and Figure S1); deletion of the other NLSs had no effect on nuclear localization. Three candidate NLSs were sufficient for Cas9 localization to the nuclei (Figure 1B and Figure S1). As seen with either anti-Cas9 or anti-HA immunostaining (Figure 1C), Cas9 nuclear localization was the most intense and prevalent with the 34-amino acid C-terminal NLS from the *Giardia* protein GL50803_2340. Thus, we created a *Giardia* CRISPR interference (CRISPRi) expression vector using the 2340NLS fused to the C-terminus of Cas9 (Figure 1D).

The degree of CRISPRi-mediated knockdown of exogenously expressed NanoLuc depends on gRNA position*.*

To determine the magnitude of gene repression using CRISPRi in *Giardia,* we created a strain that constitutively expresses NanoLuc (NLuc), a small and bright luciferase reporter (60), under

the control of the *Giardia* MDH promoter. Due to the small size of NLuc (19.1 kDa, 513 bp) we designed one gRNA to target the transcriptional start site (TSS) (-11) and 10 gRNAs to target the entire coding region at 50 base-pair intervals (+53, +95, +147, +193, +255, +285, +365, +401, +444, +488) (Figure 2A). This robust sampling of gRNA positioning allowed us to evaluate how the target position of the gRNA can affect overall repression via CRISPRi. The gRNA that targets the TSS (NLuc(-11)) did not effectively repress NLuc luminescence. However, eight of 10 gRNAs that target within the coding region repressed NLuc luminescence by ~18-87% compared to the NanoLucNeo strain with no dCas9 or gRNA expression (Figure 2B). Maximal repression occurred with NLuc+255 and NLuc+488 gRNAs (~86% and ~87% decrease in luminescence, respectively) (Figure 2B).

CRISPRi mediated knockdown of kinesin-13 causes significant increases in flagellar length

To determine the efficiency of CRISPRi knockdown of endogenous genes in *Giardia,* we designed four gRNAs (-61, -55, +24, +60) to target kinesin-13 (GiardiaDB GL50803_16945), a motor protein that regulates microtubule depolymerization dynamics. *Giardia* has four pairs of bilaterally symmetric flagellar pairs that are maintained at four different lengths (Figure 3A) by intraflagellar transport (IFT). The length of a flagellum is determined by the balance of kinesin-2 dependent assembly and kinesin-13 dependent disassembly at the distal flagellar tip (31). The overexpression of a dominant-negative kinesin-13 rigor mutant causes significant increases in the length of *Giardia's* eight flagella, larger median bodies, and cell division defects (31).

To assess the efficiency of kinesin-13 knockdown, we fixed cells and measured the length of the caudal flagella, a convenient reporter for flagellar length (31). gRNAs targeted to the coding region of kinesin-13 (K13+24, K13+60) increased the length of caudal flagella by ~12 and 25% when compared to a control strain expressing dCas9 with no gRNA (Figure 3B,C). Targeting dCas9 with gRNAs to the promoter region (-61, -55) did not significantly affect flagellar length (Figure 3B), similar to our observations of gRNAs targeting the promoter regions of NLuc (Figure 2).

To determine the degree of transcriptional repression conferred by CRISPRi knockdown, we quantified the expression of kinesin-13 in the K13+60 and no gRNA strains using quantitative PCR (qPCR). Kinesin-13 expression was reduced by ~59% in the K13+60 strain as compared to the no gRNA control (Figure 3D).

Lastly, to assess the penetrance of CRISPRi silencing in *Giardia,* we fixed and stained the K13+60 and no gRNA control strains with an anti-Cas9 antibody. dCas9 had no effect on the caudal flagellar length of no gRNA control cells. The severity of the flagellar length phenotype was directly correlated with trophozoites that have nuclei with positive dCas9 staining (Figure 3E). Cells with detectable dCas9 staining in their nuclei had caudal flagella that were ~33% longer than control cells, while cells negative for dCas9 staining were only ~11% longer than no gRNA control strains (Figure 3F).

Tuning the efficiency of kinesin-2a knockdowns with multiple gRNAs

Giardia possesses a single heterotrimeric kinesin-2 motor, consisting of kinesin-2a, 2b, and the kinesin-associated protein (KAP), that is required for flagellar assembly and maintenance (32). Both morpholino-based knockdown of kinesin-2b and dominant negative expression of a rigor mutant kinesin-2a result in significant flagellar shortening and mitotic defects (32). Therefore, to test whether multiple gRNAs increased the knockdown efficiency, we compared the degree of kinesin-2a (GiardiaDB GL50803_17333) knockdown using either single (+127) or double gRNA (+127, +42) cassettes (Figure 3A).

Expression of K2+127 reduced caudal flagellar length by ~42% as compared to the no gRNA control (Figure 4C,D), whereas K2+127/+42 expression reduced caudal flagellar length by ~33% compared to the dual no gRNA control strain (Figure 4C,D). To confirm that these phenotypes were due to decreased expression of kinesin-2a, we quantified the degree of kinesin-2a repression for K2+127 and K2+127/42 knockdowns and noted that K2+127 decreased kinesin-2a expression by ~59% compared to the no gRNA control. Kinesin-2a expression was decreased ~50% in the K2+127/+42 knockdown as compared to the dual no gRNA control strain (Figure 4B). The growth rates of strains expressing dCas9 in the absence of gRNAs are similar to wild-type.

Knockdown of a disc-associated protein causes severe ventral disc structural defects

Attachment to the host intestinal epithelium by the ventral disc – a highly ordered and complex microtubule (MT) array – is critical to *Giardia*'s pathogenesis in the host (61). The disc is defined by more than 90 parallel and uniformly spaced MTs that spiral one and a quarter turns into a

domed structure (62-67). Disc MTs terminate with their plus ends either on the periphery of the disc or in the “overlap zone”, the region of overlap between the upper and lower portions of the disc spiral (61). MBP (GiardiaDB GL50803_16343) is one of almost 90 disc associated proteins that localize to the disc (61), with particular localization to the overlap zone (35). Morpholino knockdown of MBP results in discs with an “open” and “flattened” conformation as well as decreased attachment efficiency (35).

To test the knockdown efficiency of MBP using CRISPRi, we created three strains with different gRNAs targeting coding and non-coding regions of the MBP gene – MBP(-7), MBP+11, and MBP+1566. The severity and penetrance of disc structural phenotypes in the three MBP knockdown strains was correlated to the presence of nuclei positive for dCas9 staining (Figure 5A). The majority of trophozoites with dCas9-positive nuclei had severe disc structural defects, with incompletely closed, and “flattened” discs as compared to the typical domed structure (Figure 5A and (61). Specifically, sixty to one hundred percent of trophozoites with dCas9 staining have aberrant disc structures using any of the three gRNAs (Figure 5B). Discs in the no gRNA controls strains had no structural defects and were comparable to wild-type (Figure 5C). Super resolution imaging using structured illumination microscopy (SIM) highlights the disrupted and open disc ultrastructure in the CRISPRi knockdowns (Figure 5C), with some cells lacking the overlap zone or larger components of the disc. Other severe defects include the fragmentation of the ventral disc and mislocalization of beta-giardin (Figure 5C), a key component of the ventral disc (61).

DISCUSSION

CRISPRi has been shown to be a robust alternative to RNAi-mediated gene silencing for precise knockdown of gene expression in both eukaryotic and bacterial model systems (37, 68). While CRISPR/Cas9-mediated knockout strategies have recently been implemented for genome engineering in several parasitic protists (69), this is the first demonstration of CRISPRi-mediated transcriptional repression in a non-model eukaryotic organism.

Our successful use of CRISPRi to repress both exogenous (Figure 2) and endogenous genes (Figures 3-5) in the "double diploid" binucleate *Giardia* underscores the versatility of this stable, modular, and tunable gene regulation system. In *Giardia*, targeting of the Cas9 or dCas9/gRNA DNA recognition complex to both nuclei (Figure 1A-C) required the addition of a native *Giardia* NLS. The *Giardia* CRISPRi expression system is compact and self-contained on a single episomal plasmid (Figure 1D). Expression of the modular dCas9 and gRNA CRISPRi cassettes does not require *Giardia* host or viral factors as is required for antisense (70) or hammerhead ribozyme-mediated transcriptional repression (71, 72). Molecular genetic tool development in *Giardia* has focused on transcriptional repression by the overexpression of long double-stranded RNAs or hammerhead ribozymes (71, 72) or by translational repression (73). Stable, robust CRISPRi-based gene regulation of single or multiple genes will transform the study of molecular and cellular biology and pathogenesis in *Giardia*.

Once imported into the nuclei, the Cas9/gRNA complex is targeted to a specific genomic locus where it sterically interferes with RNA polymerase or transcription factor binding or with transcriptional elongation, as has been shown in bacteria or other eukaryotes (37). The ability to direct dCas9 or even other native transcriptional elements to both nuclei *in Giardia* will enable the modulation of transcriptional networks not only by repression, but also by differential expression or overexpression through the fusion of dCas9 to *Giardia*-specific transcription factors or enhancers (68).

Stable transcriptional repression of exogenous or endogenous genes with single or multiple gRNAs

The choice of gRNA target site has been shown to impact the degree of transcriptional repression in every CRISPRi system (37). In some bacterial systems, targeting gRNAs close to the TSS results in stronger repression, whereas this trend has not been seen in human cells (27, 74). To determine how gRNA positioning might influence the magnitude of transcriptional repression in *Giardia,* we systematically targeted NLuc, a luminescent reporter gene, with 11 different gRNAs designed to target the transcriptional start site and the coding regions of gene with 50-bp frequency. Our results show that various gRNA positions provide substantial repression of NanoLuc luminescence; however, there was no correlation between gRNA position and the magnitude of repression. While our interpretation is limited due to the ability to design only a single gRNA to the TSS and the inability to target the native promoter (MDH) used to drive NLuc expression (without also affecting the expression of the *Giardia* MDH gene and the expression of dCas9 itself), the targeting of kinesin-13 promoter and coding regions

provide further support for this conclusion. Thus we recommend that at least several gRNAs for each target be tested for successful gene repression in *Giardia,* as has been suggested CRISPRi in human cells (74). Furthermore, the absence of significant repression using gRNAs that target the promoter and TSS of NLuc and kinesin-13 and the robust silencing observed with gRNAs that target the coding regions of these genes suggest that efficient repression in *Giardia* occurs by the inhibition of transcriptional elongation, rather than inhibition of transcriptional initiation. (37).

Interrogating key aspects of Giardia's life cycle and basic biology using CRISPRi

Giardia has a two-stage life cycle in which infectious cysts are first ingested from contaminated food or water (75). After passage through the stomach, cysts develop into motile trophozoites that attach to intestinal epithelium via the ventral disc. Trophozoites proliferate in the small intestine, later transforming into cysts that are shed and disseminated into the environment. *Giardia's* dynamic and elaborated microtubule cytoskeleton – including the ventral disc (61), the eight flagella (76), the median body, and two mitotic spindles – is of critical importance throughout both stages of its life cycle (75, 77). This study represents the first use of transcriptional repression to disrupt cytoskeletal function in *Giardia*. Our demonstration of CRISPRi-mediated stable transcriptional repression of three endogenous cytoskeletal proteins (Figures 3-5) highlights the versatility of this method to interrogate *Giardia* microtubule functioning in motility and attachment.

Motile trophozoites colonize and proliferate in the gastrointestinal tract (76), attaching extracellularly to the intestinal villi, and resisting peristalsis using the ventral disc (75, 78). Flagellar motility may be important for early stages in parasite positioning in the host (33), and for other aspects of *Giardia*'s life cycle including cytokinesis (29, 32, 79), and excystation (80). Flagellar growth and length maintenance are dependent upon intraflagellar transport (IFT) to supply building blocks to the distal flagellar tips, the site of assembly (81). In terms of flagellar growth and assembly, the heterotrimeric kinesin-2 complex is present in *Giardia* and has conserved functions in assembly of external regions of axonemes (31). Kinesin-13 regulates flagellar length in all giardial axonemes through the promotion of microtubule disassembly at the distal flagellar tips (82). Overexpression of dominant negative kinesin-2 or kinesin-13 thus results in aberrant flagellar lengths of all of the eight flagella (31, 32). We confirm similar length defects with CRISPRi knockdowns of kinesin-2a (Figure 3) and kinesin-13 (Figure 4), supporting the essential roles of these two kinesins in flagellar length regulation in *Giardia*.

As noted with transcriptional repression of the NanoLuc reporter (Figure 2), the degree of CRISPRi knockdown phenotypes of kinesin-13 and MBP (Figures 3 and 5) are contingent upon the targeting position of the gRNA and the presence of dCas9 in the nuclei. Population level assessments of the degree of transcriptional knockdowns range from 10 to 59%, however more severe phenotypes are associated dCas9 positive cells than dCas9 negative cells (Figure 3). Therefore CRISPRi permits the creation of a gradation of phenotypes for our endogenous targets that are dependent on the gRNA being used. The variations in knockdown levels highlight the overall tunability of this system for knockdown of endogenous genes in contrast to

transient morpholino knockdown (30, 73), and underscore the requirement for dCas9 localization and expression in the nuclei. Tunable phenotypes, with less than complete transcriptional repression, are critical toward to the evaluation of essential *Giardia* genes. Our modular design of the *Giardia* gRNA expression cassette allows for concatenation of more than one gRNA to target multiple sites on one target gene (Figure 3), or to target more than one *Giardia* gene or gene family.

Giardia's ventral disc is composed of nearly 90 proteins, and morpholino knockdown of the disc-associated protein DAP16343 (median body protein, or MBP) results in discs with an open and flattened conformation and significant attachment defects (35). Stable CRISPRi-mediated knockdown of MBP (Figure 5) resulted in the same "open" and "flat" disc phenotype observed using transient morpholino translational knockdowns (35), supporting the use of CRISPRi to affect disc structure and attachment. In contrast to morpholinos, the MBP knockdown strain is stable and Cas9+ phenotypes are 60-100% penetrant, and therefore more amenable to *in vitro* analysis of defects in disc structure or attachment. The use of FACS and other methods to enrich for trophozoites strongly express dCas9 could increase the effect size for this method, as has been seen in other CRISPRi systems (74).

Genome-wide CRISPRi functional screens of novel proteins in Giardia

The *Giardia* WBC6 genome contains roughly 6000 genes (15), with over 3500 expressed in trophozoites and 2500 expressed in cysts (83). Much of the *Giardia* genome encodes "hypothetical" proteins that lack similarity to proteins in other organisms, and more

importantly, lack homology to proteins in the human host, and thus could serve as potential druggable targets (15). For example, more than half of known proteins associated with the ventral disc lack homology to proteins in other eukaryotes, or merely possess simple protein interaction motifs (36). Similarly, some of the most highly expressed genes in *in vivo* encysting parasites are proteins with no known function (84).

CRISPRi will rapidly change how we study basic cell biology, development, and pathogenesis of this widespread and understudied parasite. Targeted or directed approaches to identify and validate candidate druggable *Giardia* proteins have generally been deprioritized due to the inability to evaluate mutant phenotypes of specific candidates. The ability to rapidly create stable knockdown strains for vital pathogenicity factors that contribute to motility and attachment using CRISPRi allows us to finally prioritize candidate *Giardia* proteins and pathways as druggable targets. Such a targeted drug development approach will change the way researchers identify, validate, and evaluate candidate proteins for anti-*Giardia* drugs. Furthermore, the use of random gRNAs for stable and inducible CRISPRi knockdowns have been used in untargeted forward genome-wide screens in bacteria (37, 85, 86) and eukaryotes (37, 68). CRISPRi would be an inexpensive and fruitful strategy to identify essential genes associated with key aspects of *Giardia's* life cycle and pathogenesis, such as attachment (61), motility (76), or encystation (84, 87).

Rapid and stable genetic manipulation of *Giardia* gene expression also permits the analysis of infection dynamics using CRISPRi knockdown parasites. We have also recently developed bioluminescent imaging (BLI) of luciferase-expressing *Giardia* strains to monitor temporal and spatial patterns of infection dynamics and metabolism in the host (36). The ability to create stable CRISPRi knockdowns in these luciferase bioreporter strains will be essential toward the understanding the cellular roles of *Giardia* proteins during colonization and encystation in the host. Combined with BLI, CRISPRi will enable the examination of fitness, colonization, or encystation differences in knockdown *Giardia* strains.

ACCESSION NUMBERS

Giardia CRISPRi vectors have been deposited in GenBank with the following accession numbers: dCas9g1pac (MH037009), NanoLucNeo (MH037010), pcGFP1Fpac (MH048881).

ACKNOWLEDGEMENTS

This work was supported by the NIH/NIAID awards R01AI077571 and R21AI119791-01 to SCD. Plasmids JDS246 (Addgene #43861) and MSP712 (Addgene #65768) were gifts from Keith Joung. Plasmid pKS_mNeonGreen-N11_NEO was a gift from Alex Paredez (University of Washington, Seattle).

FIGURE LEGENDS

Figure 1. ***A Giardia NLS is necessary and sufficient to localize Cas9 and dCas9 to both nuclei.*** Neither a single C-terminal nor dual N- and C-terminal SV40 nuclear localization signals (NLSs) are sufficient for localization Cas9-GFP to either or both nuclei in *Giardia*. Cas9 with the SV40NLS localizes only to the cytoplasm with no detectable signal in either nucleus (A). A native 34-amino acid C-terminal NLS from the *Giardia* protein GL50803_2340 (2340NLS) is necessary for the nuclear localization of 2340 to both nuclei (B). Deleting the 2340NLS from its native protein abolishes nuclear localization in the 2340GFP fusion strain. In C, the addition of the 2340NLS to the C terminus of the Cas9 or catalytically inactive Cas9 (dCas9) is sufficient for nuclear localization to both nuclei as shown by anti-Cas9 or anti-HA immunostaining. Panel D shows a schematic of *Giardia* CRISPRi vector dCas9g1pac, with dCas9 with a C-terminal 2340NLS and a 3XHA epitope tag driven by the malate dehydrogenase promoter (PMDH), as well as the gRNA cassette driven by the U6 spliceosomal RNA pol III promoter. The gRNA cassette includes inverted BbsI restriction sites for rapid cloning of annealed oligonucleotides encoding the specific gRNAs (Methods).

Figure 2. ***The degree of CRISPRi-mediated knockdown of exogenously expressed NanoLuc in Giardia depends on gRNA position.*** Eleven guide RNAs (gRNAs) were designed to examine the contribution of gRNA position to CRISPRi-mediated knockdown of NanoLuc using luminescence as a reporter of knockdown efficiency (Methods). The first gRNA (NLuc(-11)) targets the transcriptional start site while the remaining ten gRNAs target the coding region of NanoLuc

(A). Only guide RNAs targeting the coding region cause in efficient repression (18-87%) of NanoLuc luminescence (B) as compared to controls lacking a guide RNA.

Figure 3. *CRISPRi mediated knockdown of kinesin-13 causes significant increases in flagellar length.* *Giardia* has four pairs of bilaterally symmetric flagella (anterior flagella (AF), ventral flagella (VF), posteriolateral flagella (PF), and caudal flagella (CF)) with distinct equilibrium interphase lengths (A). CRISPRi-mediated knockdown of endogenous kinesin-13 was examined using one of four gRNAs targeting either the promoter or coding regions (B). Significant increases in caudal flagellar length are seen in knockdowns with gRNAs targeting only the coding region (K13+24, K13+60). Caudal flagellar length is unaffected by gRNAs (K13(-61) and K13(-55)) that target the promoter region. Representative caudal flagellar length increases with CRISPRi K13+60 knockdown strain are seen with differential interference contrast (DIC) image (C). Quantitative PCR (qPCR) analysis of K13+60 indicates that transcription of kinesin-13 is reduced by 59% compared to the no gRNA control strain (D). To evaluate penetrance of the kinesin-13 knockdown (E), K13+60 trophozoites were immunostained to determine flagellar length in dCas9 positive (top) and negative (bottom) cells using anti-Cas9 and anti-alpha tubulin antibodies. dCas9 positive cells in the K13+60 knockdown strain had an increased severity of caudal length changes as compared to dCas9 negative cells (F).

Figure 4. *CRISPRi knockdown of kinesin-2a using single or multiple gRNAs*. CRISPRi-mediated knockdown of a second endogenous kinesin involved in flagellar length regulation – kinesin-2a – was evaluated by expressing either a single gRNA (K2+127) or dual gRNAs (K2+127/+42) by

modifying the gRNA cassette to include a SacI site for the addition of gRNA cassettes in tandem (see schematic, A). The degree of knockdown was slightly higher in the strain (K2+127/+42) expressing the dual gRNAs (about 59%) than in the strain (K2+127) expressing the single gRNA when normalized the constitutive GAPDH gene (B). Expression of a dominant negative kinesin-2 causes significant decreases in flagellar length, and CRISPRi-mediated knockdown of kinesin-2a using either single (K2+127) or dual gRNAs (K2+127/+42) results in significant flagellar shortening of the caudal flagella as shown by DIC imaging (C). Similar relative caudal length differences (about 30-40% shorter than wild-type) were observed using single or dual gRNAs (D).

Figure 5. ***CRISPRi knockdown of the ventral disc protein MBP causes severe structural defects***

Each of the gRNAs targeting the promoter (MBP(-7)) or coding region (MBP+11, MBP+1566) of the disc-associated the median body protein (MBP, or DAP16343) result in the same "open" disc conformation seen with morpholino knockdown of MBP (35). Immunostaining with the disc-specific antibody anti-β-giardin enables the visualization of the disc. dCas9-positive cells are quantified using anti-Cas9 immunostaining, and the presence of dCas9 strongly correlates with aberrant ventral discs in all MBP knockdown strains (A). For all knockdown strains, between 60-100% of Cas9 positive cells had aberrant disc phenotypes (B). Super-resolution SIM imaging of the MBP +11 knockdown strain illustrates the severe defects in ventral disc structure including the lack of the overlap zone and opening of the disc (red arrows) and mislocalization of beta-giardin (blue arrow), a component of the ventral disc microribbons, as compared to strains lacking a gRNA (C).

Supplemental Figure 1. ***Evaluation of two alternative Giardia nuclear localization signals for Cas9 localization to nuclei.*** To test the ability of predicted NLSs from two alternative nuclear-localizing *Giardia* proteins (GL50803_6366 and GL50803_10370) to target Cas9 to the two nuclei, we first deleted the predicted NLS(s) in a C-terminal GFP-tagged strain (6366GFP or 10370GFP). While some decrease in nuclear localization was observed after deletion of the 6366NLS, GFP signal remained in the nuclei, indicating that this NLS was not necessary for nuclear targeting. Deletion of the 10370 NLS had a greater effect, as there was GFP localization to the cytoplasm. Fusion of either the 6366NLS or the 10370NLS to the C terminus of Cas9, resulted in some nuclear localization of Cas9 as confirmed by immunostaining. However, Cas9 nuclear localization was found in a lower proportion of cells than with the 2340NLS (Figure 1), and the 10370NLS in particular was not sufficient to target Cas9 to both nuclei in a majority of cells.

Supplemental Figure 2. ***NanoLuc bioluminescence is directly correlated with cell density.*** Relative bioluminescence (Y axis) of NanoLuc-expressing strains is plotted with increasing cell density (X axis) to evaluate correlation of luminescence with cell density.

Supplemental Table 1. ***Sequence of oligonucleotides used for gRNA cloning.*** This table lists the two oligonucleotides annealed together and ligated into CRISPRi vectors to generate the gRNA for knockdowns of NanoLuc (Figure 2), kinesin-13 (Figure 3), kinesin-2 (Figure 4) and MBP (Figure 5) with the corresponding PAM sequences.

REFERENCES

1. Savioli L, Smith H, Thompson A. 2006. *Giardia* and *Cryptosporidium* join the 'Neglected Diseases Initiative'. Trends Parasitol 22:203-208.

2. Troeger H, Epple HJ, Schneider T, Wahnschaffe U, Ullrich R, Burchard GD, Jelinek T, Zeitz M, Fromm M, Schulzke JD. 2007. Effect of chronic Giardia lamblia infection on epithelial transport and barrier function in human duodenum. Gut 56:328-35.

3. Flanagan PA. 1992. Giardia--diagnosis, clinical course and epidemiology. A review. Epidemiol Infect 109:1-22.

4. Upcroft P, Upcroft JA. 2001. Drug targets and mechanisms of resistance in the anaerobic protozoa. Clinical Microbiology Reviews 14:150-164.

5. Land KM, Johnson PJ. 1999. Molecular basis of metronidazole resistance in pathogenic bacteria and protozoa. Drug Resist Updat 2:289-294.

6. Barat LM, Bloland PB. 1997. Drug resistance among malaria and other parasites. Infect Dis Clin North Am 11:969-87.

7. Upcroft J, Samarawickrema N, Brown D, Upcroft P. 1996. Mechanisms of metronidazole resistance in *Giardia* and *Entamoeba*. Abstracts of the Interscience Conference on Antimicrobial Agents and Chemotherapy 36:47.

8. Bartelt LA, Sartor RB. 2015. Advances in understanding Giardia: determinants and mechanisms of chronic sequelae. F1000Prime Rep 7:62.

9. Heyworth MF. 2014. Immunological aspects of Giardia infections. Parasite 21:55.

10. Bernander R, Palm JE, Svard SG. 2001. Genome ploidy in different stages of the Giardia lamblia life cycle. Cell Microbiol 3:55-62.

11. Kabnick KS, Peattie DA. 1990. In situ analyses reveal that the two nuclei of Giardia lamblia are equivalent. J Cell Sci 95 (Pt 3):353-60.

12. Franzen O, Jerlstrom-Hultqvist J, Castro E, Sherwood E, Ankarklev J, Reiner DS, Palm D, Andersson JO, Andersson B, Svard SG. 2009. Draft genome sequencing of *Giardia intestinalis* assemblage B isolate GS: is human giardiasis caused by two different species? PLoS Pathog 5:e1000560.

13. Adam RD, Dahlstrom EW, Martens CA, Bruno DP, Barbian KD, Ricklefs SM, Hernandez MM, Narla NP, Patel RB, Porcella SF, Nash TE. 2013. Genome sequencing of Giardia lamblia genotypes A2 and B isolates (DH and GS) and comparative analysis with the genomes of genotypes A1 and E (WB and Pig). Genome Biol Evol 5:2498-511.

14. Hanevik K, Bakken R, Brattbakk HR, Saghaug CS, Langeland N. 2015. Whole genome sequencing of clinical isolates of Giardia lamblia. Clin Microbiol Infect 21:192 e1-3.

15. Morrison HG, McArthur AG, Gillin FD, Aley SB, Adam RD, Olsen GJ, Best AA, Cande WZ, Chen F, Cipriano MJ, Davids BJ, Dawson SC, Elmendorf HG, Hehl AB, Holder ME, Huse

SM, Kim UU, Lasek-Nesselquist E, Manning G, Nigam A, Nixon JE, Palm D, Passamaneck NE, Prabhu A, Reich CI, Reiner DS, Samuelson J, Svard SG, Sogin ML. 2007. Genomic minimalism in the early diverging intestinal parasite *Giardia lamblia*. Science 317:1921-6.

16. DiCarlo JE, Norville JE, Mali P, Rios X, Aach J, Church GM. 2013. Genome engineering in Saccharomyces cerevisiae using CRISPR-Cas systems. Nucleic Acids Res 41:4336-43.

17. Hwang WY, Fu Y, Reyon D, Maeder ML, Tsai SQ, Sander JD, Peterson RT, Yeh JR, Joung JK. 2013. Efficient genome editing in zebrafish using a CRISPR-Cas system. Nat Biotechnol 31:227-9.

18. Wang H, Yang H, Shivalila CS, Dawlaty MM, Cheng AW, Zhang F, Jaenisch R. 2013. One-step generation of mice carrying mutations in multiple genes by CRISPR/Cas-mediated genome engineering. Cell 153:910-8.

19. Mali P, Yang L, Esvelt KM, Aach J, Guell M, DiCarlo JE, Norville JE, Church GM. 2013. RNA-guided human genome engineering via Cas9. Science 339:823-6.

20. Bedell VM, Wang Y, Campbell JM, Poshusta TL, Starker CG, Krug RG, 2nd, Tan W, Penheiter SG, Ma AC, Leung AY, Fahrenkrug SC, Carlson DF, Voytas DF, Clark KJ, Essner JJ, Ekker SC. 2012. In vivo genome editing using a high-efficiency TALEN system. Nature 491:114-8.

21. Clark KJ, Voytas DF, Ekker SC. 2011. A TALE of two nucleases: gene targeting for the masses? Zebrafish 8:147-9.

22. Poxleitner MK, Carpenter ML, Mancuso JJ, Wang CJ, Dawson SC, Cande WZ. 2008. Evidence for karyogamy and exchange of genetic material in the binucleate intestinal parasite Giardia intestinalis. Science 319:1530-3.

23. Elmendorf HG, Singer SM, Nash TE. 2000. Targeting of proteins to the nuclei of Giardia lamblia. Mol Biochem Parasitol 106:315-9.

24. Ebneter JA, Heusser SD, Schraner EM, Hehl AB, Faso C. 2016. Cyst-Wall-Protein-1 is fundamental for Golgi-like organelle neogenesis and cyst-wall biosynthesis in Giardia lamblia. Nat Commun 7:13859.

25. Davis-Hayman SR, Nash TE. 2002. Genetic manipulation of Giardia lamblia. Mol Biochem Parasitol 122:1-7.

26. Gourguechon S, Cande WZ. 2011. Rapid tagging and integration of genes in Giardia intestinalis. Eukaryotic Cell 10:142-5.

27. Qi LS, Larson MH, Gilbert LA, Doudna JA, Weissman JS, Arkin AP, Lim WA. 2013. Repurposing CRISPR as an RNA-guided platform for sequence-specific control of gene expression. Cell 152:1173-83.

28. Horlock-Roberts K, Reaume C, Dayer G, Ouellet C, Cook N, Yee J. 2017. Drug-Free Approach To Study the Unusual Cell Cycle of Giardia intestinalis. mSphere 2.

29. Hardin WR, Li R, Xu J, Shelton AM, Alas GCM, Minin VN, Paredez AR. 2017. Myosin-independent cytokinesis in Giardia utilizes flagella to coordinate force generation and direct membrane trafficking. Proc Natl Acad Sci U S A 114:E5854-E5863.

30. Krtkova J, Paredez AR. 2017. Use of Translation Blocking Morpholinos for Gene Knockdown in Giardia lamblia. Methods Mol Biol 1565:123-140.

31. Dawson SC, Sagolla MS, Mancuso JJ, Woessner DJ, House SA, Fritz-Laylin L, Cande WZ. 2007. Kinesin-13 regulates flagellar, interphase, and mitotic microtubule dynamics in Giardia intestinalis. Eukaryot Cell 6:2354-64.

32. Hoeng JC, Dawson SC, House SA, Sagolla MS, Pham JK, Mancuso JJ, Lowe J, Cande WZ. 2008. High-resolution crystal structure and in vivo function of a kinesin-2 homologue in Giardia intestinalis. Mol Biol Cell 19:3124-37.

33. House SA, Richter DJ, Pham JK, Dawson SC. 2011. Giardia flagellar motility is not directly required to maintain attachment to surfaces. PLoS Pathog 7:e1002167.

34. Paredez AR, Assaf ZJ, Sept D, Timofejeva L, Dawson SC, Wang CJ, Cande WZ. 2011. An actin cytoskeleton with evolutionarily conserved functions in the absence of canonical actin-binding proteins. Proc Natl Acad Sci U S A 108:6151-6.

35. Woessner DJ, Dawson SC. 2012. The Giardia median body protein is a ventral disc protein that is critical for maintaining a domed disc conformation during attachment. Eukaryot Cell 11:292-301.

36. Barash N, Nosala, C, Pham, JK, McInally, SG, Gourguechon, S., McCarthy-Sinclair, B, and SC Dawson. 2017. Giardia colonizes and encysts in high density foci in the murine small intestine. mSphere 2:e00343-16.

37. Larson MH, Gilbert LA, Wang X, Lim WA, Weissman JS, Qi LS. 2013. CRISPR interference (CRISPRi) for sequence-specific control of gene expression. Nat Protoc 8:2180-96.

38. Zhang B, Liu ZQ, Liu C, Zheng YG. 2016. Application of CRISPRi in Corynebacterium glutamicum for shikimic acid production. Biotechnol Lett 38:2153-2161.

39. Liu X, Gallay C, Kjos M, Domenech A, Slager J, van Kessel SP, Knoops K, Sorg RA, Zhang JR, Veening JW. 2017. High-throughput CRISPRi phenotyping identifies new essential genes in Streptococcus pneumoniae. Mol Syst Biol 13:931.

40. Tao W, Lv L, Chen GQ. 2017. Engineering Halomonas species TD01 for enhanced polyhydroxyalkanoates synthesis via CRISPRi. Microb Cell Fact 16:48.

41. Zuberi A, Misba L, Khan AU. 2017. CRISPR Interference (CRISPRi) Inhibition of luxS Gene Expression in E. coli: An Approach to Inhibit Biofilm. Front Cell Infect Microbiol 7:214.

42. Kaczmarzyk D, Cengic I, Yao L, Hudson EP. 2018. Diversion of the long-chain acyl-ACP pool in Synechocystis to fatty alcohols through CRISPRi repression of the essential phosphate acyltransferase PlsX. Metab Eng 45:59-66.

43. Saraiya AA, Wang CC. 2008. snoRNA, a novel precursor of microRNA in Giardia lamblia. PLoS Pathog 4:e1000224.

44. Zhang YQ, Chen DL, Tian HF, Zhang BH, Wen JF. 2009. Genome-wide computational identification of microRNAs and their targets in the deep-branching eukaryote Giardia lamblia. Comput Biol Chem 33:391-6.

45. Li W, Saraiya AA, Wang CC. 2011. Gene regulation in Giardia lambia involves a putative microRNA derived from a small nucleolar RNA. PLoS Negl Trop Dis 5:e1338.

46. Elmendorf HG, Singer SM, Nash TE. 2001. The abundance of sterile transcripts in Giardia lamblia. Nucleic Acids Res 29:4674-83.

47. Hudson AJ, Moore AN, Elniski D, Joseph J, Yee J, Russell AG. 2012. Evolutionarily divergent spliceosomal snRNAs and a conserved non-coding RNA processing motif in Giardia lamblia. Nucleic Acids Res 40:10995-1008.

48. Jost M, Chen Y, Gilbert LA, Horlbeck MA, Krenning L, Menchon G, Rai A, Cho MY, Stern JJ, Prota AE, Kampmann M, Akhmanova A, Steinmetz MO, Tanenbaum ME, Weissman JS. 2017. Combined CRISPRi/a-Based Chemical Genetic Screens Reveal that Rigosertib Is a Microtubule-Destabilizing Agent. Mol Cell 68:210-223 e6.

49. Hagen KD, Hirakawa MP, House SA, Schwartz CL, Pham JK, Cipriano MJ, De La Torre MJ, Sek AC, Du G, Forsythe BM, Dawson SC. 2011. Novel structural components of the ventral disc and lateral crest in Giardia intestinalis. PLoS Negl Trop Dis 5:e1442.

50. Aurrecoechea C, Brestelli J, Brunk BP, Carlton JM, Dommer J, Fischer S, Gajria B, Gao X, Gingle A, Grant G, Harb OS, Heiges M, Innamorato F, Iodice J, Kissinger JC, Kraemer E, Li W, Miller JA, Morrison HG, Nayak V, Pennington C, Pinney DF, Roos DS, Ross C,

Stoeckert CJ, Jr., Sullivan S, Treatman C, Wang H. 2009. GiardiaDB and TrichDB: integrated genomic resources for the eukaryotic protist pathogens Giardia lamblia and Trichomonas vaginalis. Nucleic Acids Res 37:D526-30.

51. Nguyen Ba AN, Pogoutse A, Provart N, Moses AM. 2009. NLStradamus: a simple Hidden Markov Model for nuclear localization signal prediction. BMC Bioinformatics 10:202.

52. Cong L, Ran FA, Cox D, Lin S, Barretto R, Habib N, Hsu PD, Wu X, Jiang W, Marraffini LA, Zhang F. 2013. Multiplex genome engineering using CRISPR/Cas systems. Science 339:819-23.

53. Kleinstiver BP, Prew MS, Tsai SQ, Topkar VV, Nguyen NT, Zheng Z, Gonzales AP, Li Z, Peterson RT, Yeh JR, Aryee MJ, Joung JK. 2015. Engineered CRISPR-Cas9 nucleases with altered PAM specificities. Nature 523:481-5.

54. Gibson DG, Young L, Chuang RY, Venter JC, Hutchison CA, 3rd, Smith HO. 2009. Enzymatic assembly of DNA molecules up to several hundred kilobases. Nat Methods 6:343-5.

55. Schindelin J, Arganda-Carreras I, Frise E, Kaynig V, Longair M, Pietzsch T, Preibisch S, Rueden C, Saalfeld S, Schmid B, Tinevez JY, White DJ, Hartenstein V, Eliceiri K, Tomancak P, Cardona A. 2012. Fiji: an open-source platform for biological-image analysis. Nat Methods 9:676-82.

56. Ball G, Demmerle J, Kaufmann R, Davis I, Dobbie IM, Schermelleh L. 2015. SIMcheck: a Toolbox for Successful Super-resolution Structured Illumination Microscopy. Sci Rep 5:15915.

57. Dawson SC, House SA. 2010. Imaging and analysis of the microtubule cytoskeleton in *Giardia*. Methods Cell Biol 97:307-39.

58. Davis JJ, Olsen GJ. 2010. Modal codon usage: assessing the typical codon usage of a genome. Mol Biol Evol 27:800-10.

59. Jiang W, Brueggeman AJ, Horken KM, Plucinak TM, Weeks DP. 2014. Successful transient expression of Cas9 and single guide RNA genes in Chlamydomonas reinhardtii. Eukaryot Cell 13:1465-9.

60. Hall MP, Unch J, Binkowski BF, Valley MP, Butler BL, Wood MG, Otto P, Zimmerman K, Vidugiris G, Machleidt T, Robers MB, Benink HA, Eggers CT, Slater MR, Meisenheimer PL, Klaubert DH, Fan F, Encell LP, Wood KV. 2012. Engineered luciferase reporter from a deep sea shrimp utilizing a novel imidazopyrazinone substrate. ACS Chem Biol 7:1848-57.

61. Nosala C, Hagen KD, Dawson SC. 2018. 'Disc-o-Fever': Getting Down with Giardia's Groovy Microtubule Organelle. Trends Cell Biol 28:99-112.

62. Feely DE, Schollmeyer JV, Erlandsen SL. 1982. *Giardia* spp.: distribution of contractile proteins in the attachment organelle. Exp Parasitol 53:145-54.

63. Crossley R, Holberton DV. 1985. Assembly of 2.5 nm filaments from giardin, a protein associated with cytoskeletal microtubules in *Giardia*. J Cell Sci 78:205-31.

64. Crossley R, Holberton DV. 1983. Characterization of proteins from the cytoskeleton of *Giardia lamblia*. J Cell Sci 59:81-103.

65. Holberton DV. 1973. Fine structure of the ventral disk apparatus and the mechanism of attachment in the flagellate *Giardia muris*. J Cell Sci 13:11-41.

66. Holberton DV. 1981. Arrangement of subunits in microribbons from *Giardia*. J Cell Sci 47:167-85.

67. Friend DS. 1966. The fine structure of *Giardia muris*. J Cell Biol 29:317-32.

68. Kampmann M. 2018. CRISPRi and CRISPRa Screens in Mammalian Cells for Precision Biology and Medicine. ACS Chem Biol 13:406-416.

69. Ren B, Gupta N. 2017. Taming Parasites by Tailoring Them. Front Cell Infect Microbiol 7:292.

70. Rivero MR, Kulakova L, Touz MC. 2010. Long double-stranded RNA produces specific gene downregulation in Giardia lamblia. J Parasitol 96:815-9.

71. Dan M, Wang AL, Wang CC. 2000. Inhibition of pyruvate-ferredoxin oxidoreductase gene expression in Giardia lamblia by a virus-mediated hammerhead ribozyme. Molecular Microbiology 36:447-456.

72. Chen L, Li J, Zhang X, Liu Q, Yin J, Yao L, Zhao Y, Cao L. 2007. Inhibition of krr1 gene expression in Giardia canis by a virus-mediated hammerhead ribozyme. Vet Parasitol 143:14-20.

73. Carpenter ML, Cande WZ. 2009. Using morpholinos for gene knockdown in *Giardia intestinalis*. Eukaryot Cell 8:916-9.

74. Gilbert LA, Larson MH, Morsut L, Liu Z, Brar GA, Torres SE, Stern-Ginossar N, Brandman O, Whitehead EH, Doudna JA, Lim WA, Weissman JS, Qi LS. 2013. CRISPR-mediated modular RNA-guided regulation of transcription in eukaryotes. Cell 154:442-51.

75. Nosala C, Dawson SC. 2015. The Critical Role of the Cytoskeleton in the Pathogenesis of Giardia. Curr Clin Microbiol Rep 2:155-162.

76. Dawson SC, House SA. 2010. Life with eight flagella: flagellar assembly and division in *Giardia*. Curr Opin Microbiol 13:480-90.

77. Dawson SC. 2010. An insider's guide to the microtubule cytoskeleton of *Giardia*. Cell Microbiol 12:588-98.

78. Elmendorf HG, Dawson SC, McCaffery JM. 2003. The cytoskeleton of *Giardia lamblia*. Int J Parasitol 33:3-28.

79. Sagolla MS, Dawson SC, Mancuso JJ, Cande WZ. 2006. Three-dimensional analysis of mitosis and cytokinesis in the binucleate parasite Giardia intestinalis. J Cell Sci 119:4889-900.

80. Boucher SE, Gillin FD. 1990. Excystation of in vitro-derived Giardia lamblia cysts. Infect Immun 58:3516-22.

81. Kozminski KG, Beech PL, Rosenbaum JL. 1995. The Chlamydomonas kinesin-like protein FLA10 is involved in motility associated with the flagellar membrane. J Cell Biol 131:1517-27.

82. Rogers GC, Rogers SL, Schwimmer TA, Ems-McClung SC, Walczak CE, Vale RD, Scholey JM, Sharp DJ. 2004. Two mitotic kinesins cooperate to drive sister chromatid separation during anaphase. Nature 427:364-70.

83. Faghiri Z, Widmer G. 2011. A comparison of the Giardia lamblia trophozoite and cyst transcriptome using microarrays. BMC Microbiol 11:91.

84. Pham JK, Nosala C, Scott EY, Nguyen KF, Hagen KD, Starcevich HN, Dawson SC. 2017. Transcriptomic Profiling of High-Density Giardia Foci Encysting in the Murine Proximal Intestine. Front Cell Infect Microbiol 7:227.

85. Hawkins JS, Wong S, Peters JM, Almeida R, Qi LS. 2015. Targeted Transcriptional Repression in Bacteria Using CRISPR Interference (CRISPRi). Methods Mol Biol 1311:349-62.

86. Quebatte M, Dehio C. 2017. Systems-level interference strategies to decipher host factors involved in bacterial pathogen interaction: from RNAi to CRISPRi. Curr Opin Microbiol 39:34-41.

87. Einarsson E, Troell K, Hoeppner MP, Grabherr M, Ribacke U, Svard SG. 2016. Coordinated Changes in Gene Expression Throughout Encystation of Giardia intestinalis. PLoS Negl Trop Dis 10:e0004571.

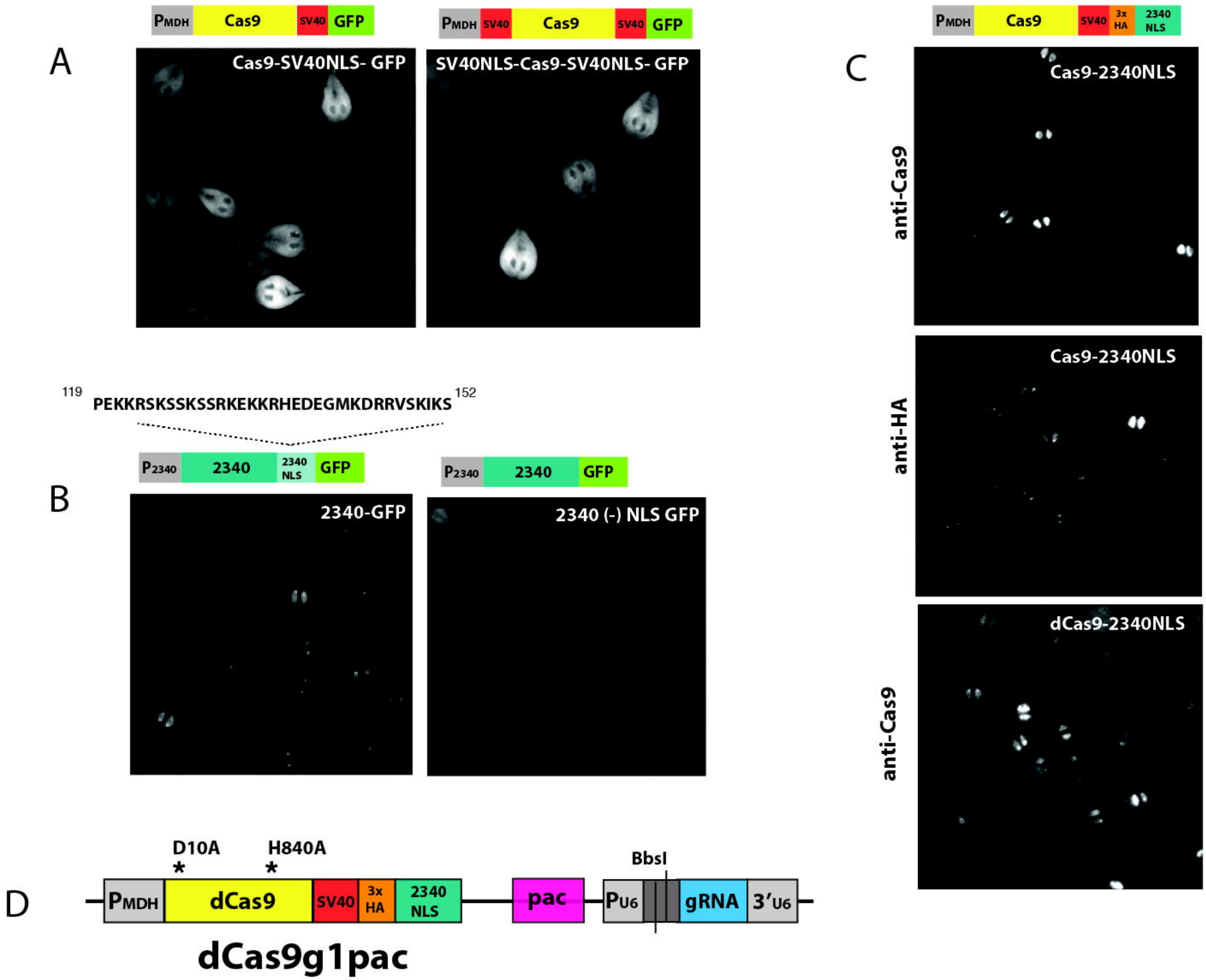
A
PMDH
Cas9
SV40
GFP
Cas9-SV40NLS- GFP
SV40NLS-Cas9-SV40NLS- GFP
B
119
PEKKRSKSSKSSRKEKKRHEDEGMKDRRVSKIKS
152
P2340
2340
2340 NLS
2340-GFP
2340 (-) NLS GFP
C
3x HA
Cas9-2340NLS
anti-Cas9
anti-HA
dCas9-2340NLS
D
D10A
H840A
dCas9
pac
BbsI
PU6
gRNA
3'U6
dCas9g1pac

A

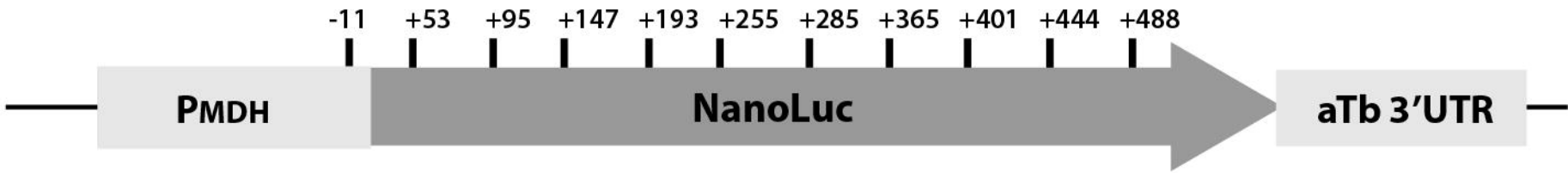
-11
+53
+95
+147
+193
+255
+285
+365
+401
+444
+488
PMDH
NanoLuc
aTb 3'UTR

B

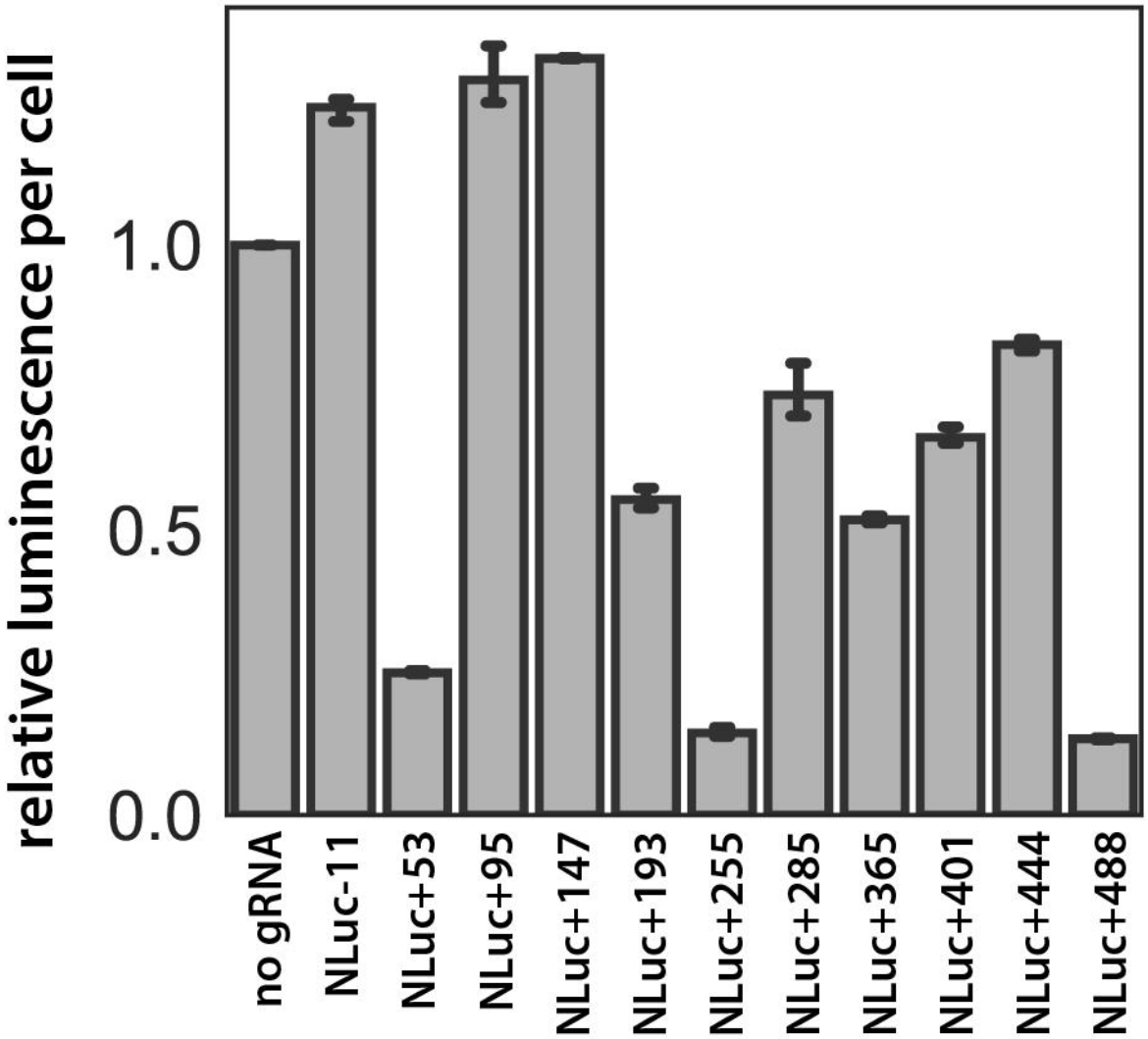
relative luminescence per cell
1.0
0.5
0.0
no gRNA
NLuc-11
NLuc+53
NLuc+95
NLuc+147
NLuc+193
NLuc+255
NLuc+285
NLuc+365
NLuc+401
NLuc+444
NLuc+488

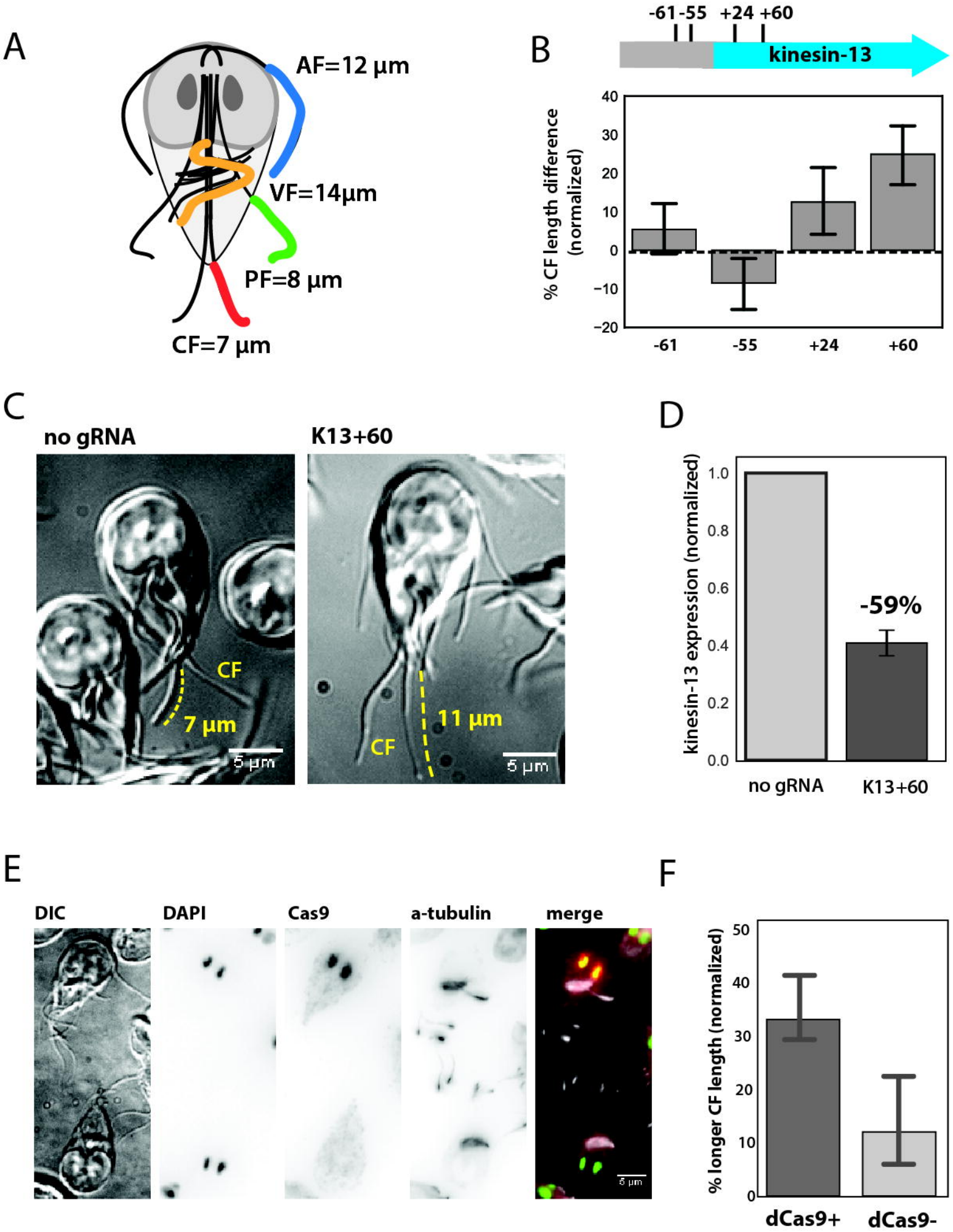
A
AF=12 µm
VF=14µm
PF=8 µm
CF=7 µm
B
-61 -55 +24 +60
kinesin-13
% CF length difference (normalized)
40
30
20
10
0
−10
−20
-61
-55
+24
+60
C
no gRNA
K13+60
CF
7 µm
5 µm
CF
11 µm
5 µm
D
kinesin-13 expression (normalized)
1.0
0.8
0.6
0.4
0.2
0.0
-59%
no gRNA
K13+60
E
DIC
DAPI
Cas9
a-tubulin
merge
5 µm
F
% longer CF length (normalized)
50
40
30
20
10
0
dCas9+
dCas9-

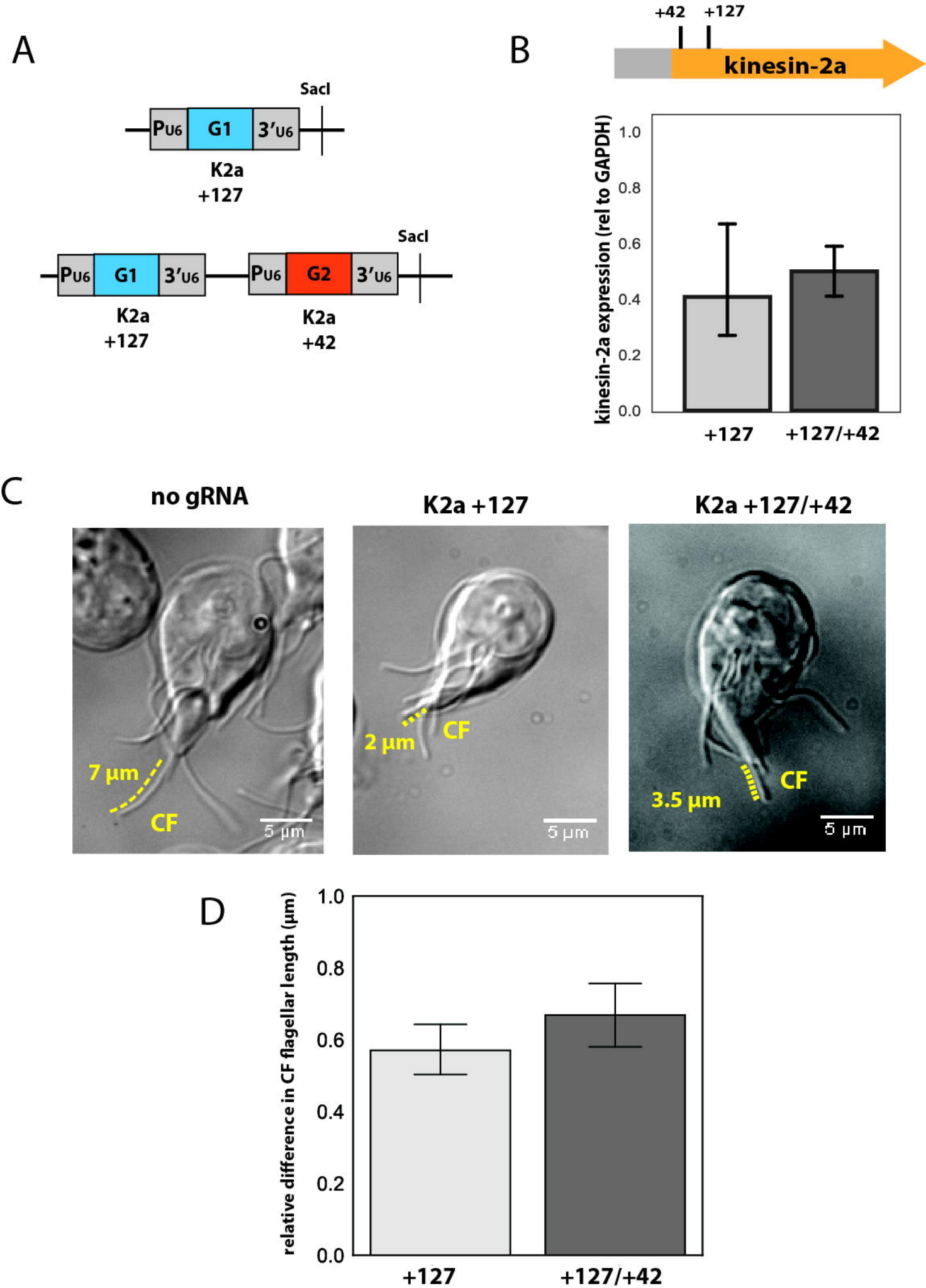
A
SacI
PU6
G1
3'U6
K2a
+127
SacI
PU6
G1
3'U6
PU6
G2
3'U6
K2a
+127
K2a
+42
B
+42
+127
kinesin-2a
kinesin-2a expression (rel to GAPDH)
1.0
0.8
0.6
0.4
0.2
0.0
+127
+127/+42
C
no gRNA
K2a +127
K2a +127/+42
7 µm
CF
5 µm
2 µm
CF
5 µm
3.5 µm
CF
5 µm
D
relative difference in CF flagellar length (µm)
1.0
0.8
0.6
0.4
0.2
0.0
+127
+127/+42

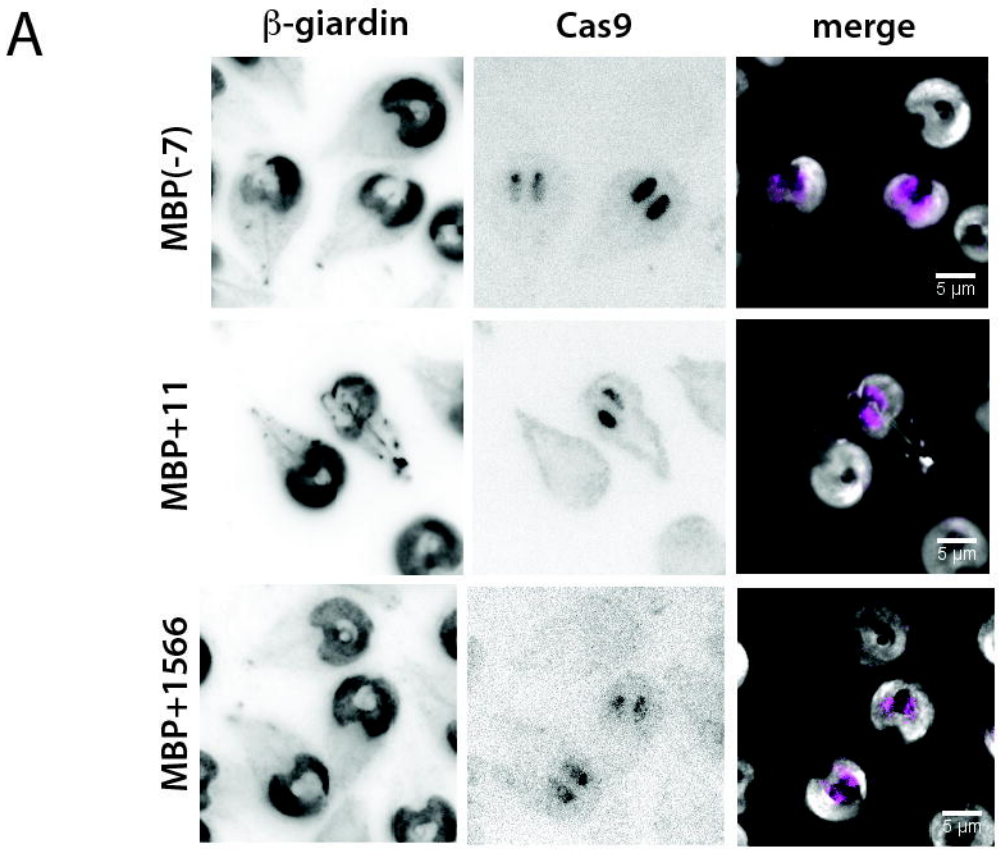
A
β-giardin
Cas9
merge
MBP(-7)
MBP+11
MBP+1566
5 µm

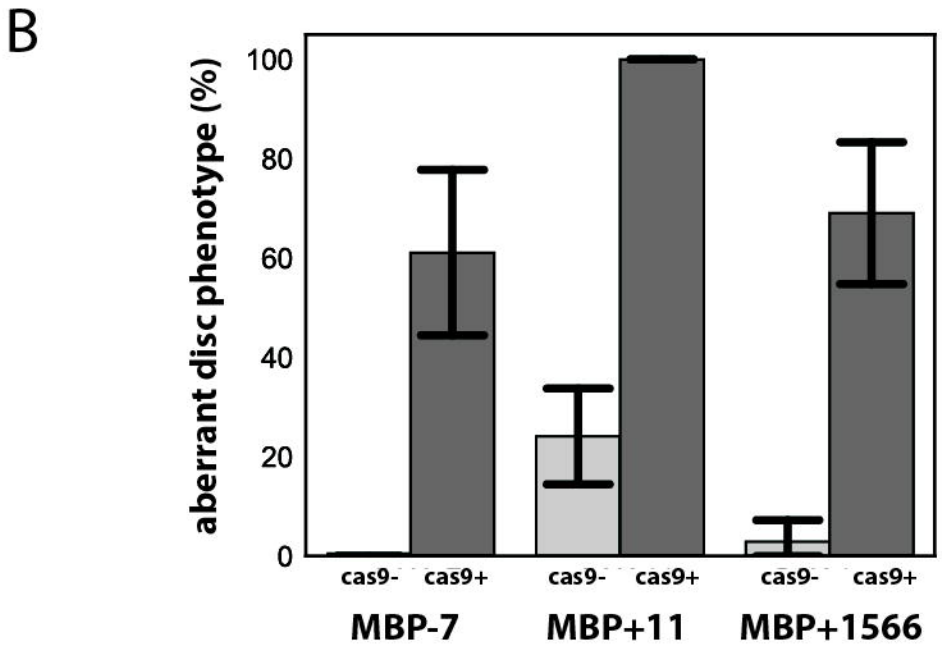
B
aberrant disc phenotype (%)
100
80
60
40
20
0
cas9-
cas9+
MBP-7
MBP+11
MBP+1566

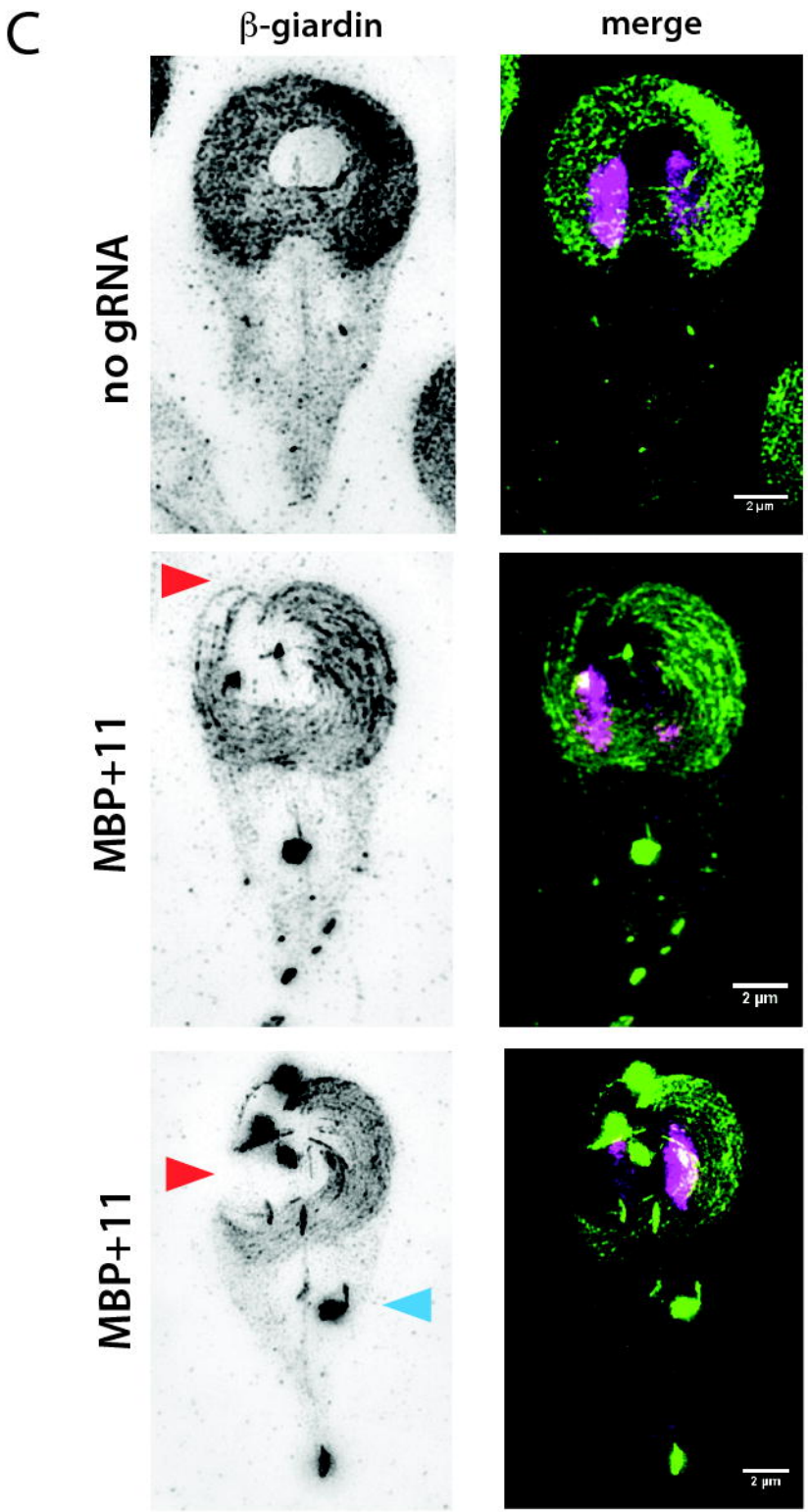
C
β-giardin
merge
no gRNA
MBP+11
MBP+11
2 µm